Supplementary material for "Topological transition in measurement-induced geometric phases"

Valentin Gebhart,[1,2,*] Kyrylo Snizhko,[2,*] Thomas Wellens,[1]
Andreas Buchleitner,[1] Alessandro Romito,[3] and Yuval Gefen[2,†]

[1] *Physikalisches Institut, Albert-Ludwigs-Universität Freiburg, Hermann-Herder-Str. 3, 79104 Freiburg, Federal Republic of Germany*
[2] *Department of Condensed Matter Physics, Weizmann Institute of Science, Rehovot 76100, Israel*
[3] *Department of Physics, Lancaster University, Lancaster LA1 4YB, United Kingdom*

(Dated: January 31, 2020)

In this supplementary material, we focus on the full distribution of trajectories and we define and study the averaged geometric phase (GP). Subsequently, we propose an experimental protocol for the detection of such an averaged phase based on Mach-Zehnder interferometry. Throughout this Supplementary material, we use the same notation introduced in the manuscript.

I. AVERAGED GEOMETRIC PHASE AND ITS TOPOLOGICAL TRANSITION

The most sensible way to define the averaged geometric phase for the full distribution of trajectories is by appealing to averaging physically measurable observables. Below, we propose a possible experimental setup for detecting the GP, which introduces a direct protocol for averaging over numerous closed trajectories. The averaged geometric phase $\bar{\chi}_{\rm geom}$ is then defined through

$$e^{2i\bar{\chi}_{\rm geom}-\alpha} := \langle e^{2i\chi_{\rm geom}}\rangle_{\rm realizations} = \sum_{\{r_k\}} \left(\langle\psi_0|\mathcal{M}_{N-1}^{(r_{N-1})}\dots\mathcal{M}_1^{(r_1)}|\psi_0\rangle\right)^2, \tag{1}$$

where $\chi_{\rm geom}$ is the geometric phase associated with each single trajectory as introduced in the paper, $e^{-\alpha}$ is a suppression factor representing the suppression of the visibility of interference in the experimental setup (cf. Section II below) and the sum extends over all possible measurement readouts $\{r_k\}$. The suppression factor accounts for two effects: (i) the probability of a successful postselection in the final strong measurement that ensures that the state trajectory is closed, and (ii) "dephasing" due to $\chi_{\rm geom}$ having a spread of values for different trajectories. The behavior of the averaged GP $\bar{\chi}_{\rm geom}$ as a function of the measurement strength has been reported in the paper (cf. Fig. (3) therein).

The dependence of the averaged GP $\bar{\chi}_{\rm geom}(\theta)$ on the polar angle θ of the measurement sequence presents a transition as a function of the measurement strength in analogy to the case of postselected measurement sequences (cf. Fig. 1). Yet, the features of the transition are different. We begin by noting that $\bar{\chi}_{\rm geom}$ is defined only $\mod \pi$ (cf. Eq. (1)) , i.e., $\bar{\chi}_{\rm geom}$ is defined on a circle S^1 of circumference π. This makes a difference for the possible values of $\bar{\chi}_{\rm geom}$ at $\theta=\pi/2$: We have $\bar{\chi}_{\rm geom}(0)=0$ as in the postelected case but at the equator $\theta=\pi/2$, where the possible values of $\chi_{\rm geom}$ are only 0 and $-\pi$, both values correspond to $e^{2i\chi_{\rm geom}}=1$ implying $\bar{\chi}_{\rm geom}(\theta=\pi/2)=0$. Hence, $\bar{\chi}_{\rm geom}(\theta)$ obeys periodic boundary conditions $\bar{\chi}_{\rm geom}(\pi/2)=\bar{\chi}_{\rm geom}(0)$, allowing us to identify the points $\theta=0$ and $\theta=\pi/2$ such that θ can be defined on a circle S^1 of circumference $\pi/2$. Therefore, $\bar{\chi}_{\rm geom}: S^1\ni\theta\mapsto\bar{\chi}_{\rm geom}\in S^1$ maps a circle onto a circle and can be classified by an integer-valued winding number m (how many times the function $\bar{\chi}_{\rm geom}(\theta)$ winds around the circle S^1 of length π as θ varies from 0 to $\pi/2$). In the limit of infinitely weak measurements, we have $\bar{\chi}_{\rm geom}(\theta)\equiv 0$, yielding $m=0$. In the limit of strong projective measurements, however, $\bar{\chi}_{\rm geom}(\theta)=\pi(\cos\theta-1)$, yielding $m=-1$. If the function $\chi_{\rm geom}(\theta)$ would depend continuously on the measurement strength, m would be preserved by increasing the measurement strength, which is incompatible with the two limiting cases of strong and infinitely weak measurements. Therefore, one expects a sharp transition at an intermediate measurement strength $c=\bar{c}_{\rm crit}$, marking the jump between these two different behaviors of $\bar{\chi}_{\rm geom}(\theta)$. At this critical measurement strength, $\bar{\chi}_{\rm geom}(\theta)$ is ill-defined for a certain polar angle $\bar{\theta}_{\rm crit}$. At these critical parameters ($\bar{\theta}_{\rm crit}\approx\pi/3$ with $c_{\rm crit}\approx 3.35$), the visibility $e^{-\alpha}$ vanishes, cf. Fig. 1 (inset).

* V.G. and K.S. contributed equally to this article.

† yuval.gefen@weizmann.ac.il

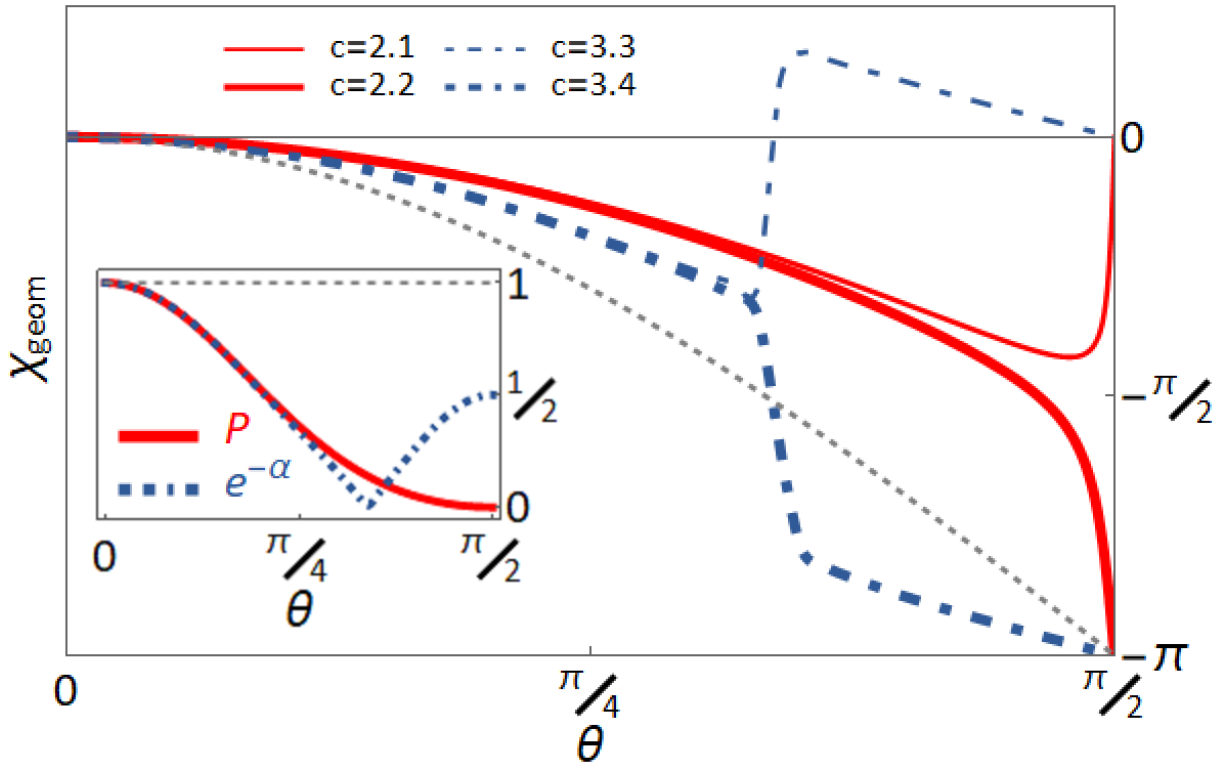

FIG. 1. **Non-monotonicity and discontinuity of averaged geometric phases**. We show the dependence of the averaged geometric phase on the polar angle θ at different values of the integrated measurement strength (cf. legend) for the averaged geometric phase (blue dot-dashed lines) compared to that of the postselected geometric phase (red solid lines). The ideal strong measurement dependence for $c \to \infty$ is presented as a grey dashed line. The dependence of the averaged GP on θ displays an abrupt transition from monotonic to non-monotonic behavior in the vicinity of $c = 3.35$. The critical strength for the averaged geometric phases differs from that of the postselected geometric phase. The behavior is underlined by the fact that $\chi_{\rm geom}(\theta)$ can assume only discrete values, 0 or $-\pi$, at $\theta = \pi/2$. Inset: The suppression factor $e^{-\alpha}$ (blue dot-dashed line) in the protocol with averaging at $c = 3.3$ compared to the probability of observing the most probable trajectory with postselected readout sequence $\{r_k = +\}$ (red solid line) at $c = 2.1$; the grey dashed line indicates $P = e^{-\alpha} = 1$ for $c \to \infty$, an asymptotic strong measurement. The plots for the protocol with averaging have been obtained by Monte Carlo simulations with $N = 500$ measurement steps per sequence and $N_{\rm realizations} = 500000$ realizations.

With the $\{r_k = +\}$ readout sequence being the most probable, one naively expects the transition to take place near $c_{\rm crit} \approx 2.15$. However, precisely at the postselected transition ($c_{\rm crit} \approx 2.15$, $\theta_{\rm crit} = \pi/2$), the probability of this readout sequence vanishes, rendering phase averaging over the remaining trajectories a crucial factor. The actual transition happens at $\bar{c}_{\rm crit} \approx 3.35$ and $\bar{\theta}_{\rm crit} \approx \pi/3$, when the contribution of the $\{r_k = +\}$ readout sequence is cancelled against the phase-averaged contribution of the remaining sequences.

II. DETECTION OF THE AVERAGED GEOMETRIC PHASE VIA MACH-ZEHNDER INTERFEROMETRY

In order to observe the averaged measurement induced GP, we propose an interferometric setup along the lines of the detection scheme described for the detection of the postselected GP in the manuscript. Here, however, a different approach to coupling the detectors to the polarization of the beam in the interferometer arms is needed. Indeed, we need to account for all readout sequences $\{r_k\}$. Given the initial detector state $+$, a readout $r_k = -$ may serve as a "which-path" detection, undermining the interference (the readout $r_k = +$ used for the postselected trajectory in the manuscript does not provide “which-path” information due to the properties of the null-type measurement we use). The only way to overcome this handicap is to couple each detector to the two interferometer arms, making it impossible to deduce from the readout signal which arm the particle went through. This is demonstrated in Fig. 2. The $k-$th detector couples to $\sigma_{\mathbf{n}_k} = \boldsymbol{\sigma} \cdot \mathbf{n}_k$ in the upper arm and to $\sigma_{-\mathbf{n}_k} = -\sigma_{\mathbf{n}_k}$ in the lower arm of the interferometer. In addition, the particle's inner degree of freedom in the lower arm is flipped before and flipped back after the sequence

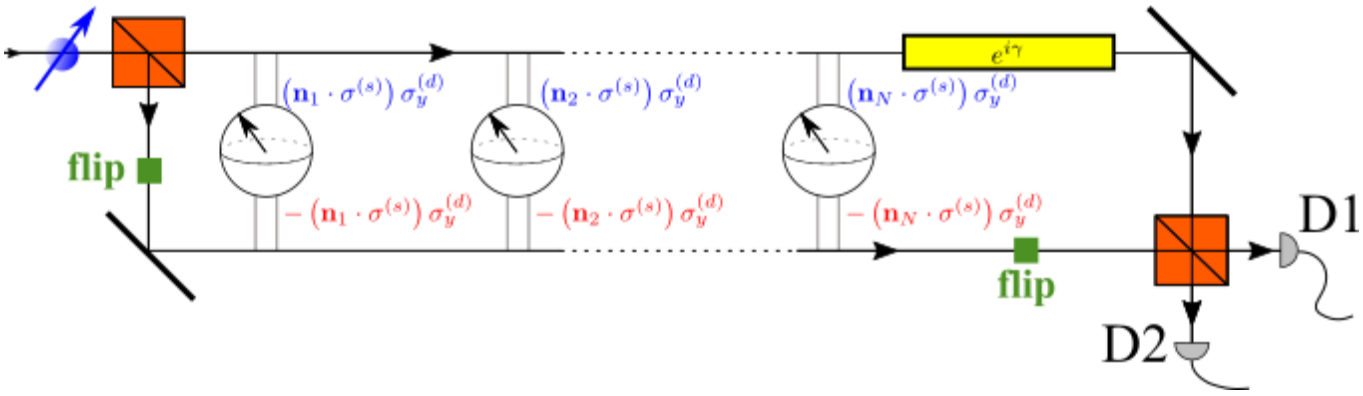

FIG. 2. **Experimental setups for observing the averaged measurement induced GPs**. Scheme for observing the averaged GP, $\bar{\chi}_{\rm geom}$, in a Mach-Zehnder interference setup. The detectors interact with the particle in both interferometer arms according to different Hamiltonians, $H_{\mathbf{n}}$ and $H_{-\mathbf{n}}$, cf. Eq. (3). Together with the flip of the particle's internal degree of freedom in the lower arm, this ensures that no "which-path" detection takes place, and all readout sequences $\{r_k\}$ contribute to the interference pattern at D1 and D2. For any given readout sequence $\{r_k\}$, the GP accumulated by the particle is opposite in the two arms of the interferometer. We assume an extra phase difference $e^{i\gamma}$ produced by means other than measurements.

of measurements. As a result, for any given readout sequence $\{r_k\}$, the trajectory on the Bloch sphere corresponding to the lower arm is exactly opposite to that of the upper arm (i.e., it is inverted with respect to the origin). It follows that the solid angle Ω subtended by the trajectories and the geometric phase $\chi_{\rm geom}$ accumulated through the upper and the lower arms have opposite signs but same magnitudes. Moreover, the probabilities $P_{\{r_k\}}$ for yielding the specific readout sequence $\{r_k\}$ are exactly the same in the two arms. This measurement scheme is thus completely devoid of "which-path" signals. Provided that the N-th measurement is postselected to yield $r_N = +$ and the runs with $r_N = -$ do not contribute to the readings at drains D1 and D2, the resulting intensities are

$$I_{1,2} = \frac{I_0}{2}\left(\sum_{\{r_k\}}\left|\langle\psi_0|\mathcal{M}_{N-1}^{(r_{N-1})}\ldots\mathcal{M}_1^{(r_1)}|\psi_0\rangle\right|^2 \pm \mathrm{Re}\sum_{\{r_k\}} e^{i\gamma}\left(\langle\psi_0|\mathcal{M}_{N-1}^{(r_{N-1})}\ldots\mathcal{M}_1^{(r_1)}|\psi_0\rangle\right)^2\right), \tag{2}$$

where the second term in the parentheses is the interference term expressible as $\mathrm{Re}\, e^{i\gamma+2i\bar{\chi}_{\rm geom}-\alpha}$ (cf. Eq. (1)). We provide a formal derivation of this result below. This *Gedankenexperiment* to detect the averaged GP could be implemented in a variety of systems, e.g., optical systems with absorptive polarizers or quantum dot detectors in electronic interferometers.

A. Output intensity of the averaged-phase interferometric detector

The observed intensity in the detection scheme presented in Fig. 2 is given by Eq. (2). This result is obtained by analyzing the evolution of the compound system-detector state across the interferometer. The collective state of the particle and all the detectors after the initial beam splitter of the interferometer is $|\Psi_i\rangle = |\psi_0\rangle\otimes[|a=1\rangle + |a=-1\rangle]\otimes|+\ldots+\rangle/\sqrt{2}$, where $a=\pm1$ describe the particle being in the upper or lower arm respectively, and $|+\ldots+\rangle$ is the initial state of all the detectors. A "flip" (cf. Fig. 2) applied at the beginning and at the end of the lower arm acts on the system via $R^{-1}(\mathbf{n}_0)\sigma_x^{(s)}R(\mathbf{n}_0)$. The interaction of the system with each of the detectors is described by the Hamiltonian

$$\tilde{H}_{\mathbf{n}_k} = \lambda(t)[1-(\mathbf{n}_k\cdot\sigma^{(s)})\sigma_z^{(a)}]\sigma_y^{(d)}/2, \tag{3}$$

where the Pauli z matrix $\sigma_z^{(a)}$ acts on the degree of freedom describing the occupation of the upper and lower arms of the interferometer. The role of $\tilde{H}_{\mathbf{n}_k}$ is to let the detector interact simultaneously with the upper and lower arms via $H_{\mathbf{n}_k}$ and $H_{-\mathbf{n}_k}$, respectively, such that the occupation of one of the two arms is not detected and ensuring that the system in the upper and the lower arms accumulate opposite geometric phases. After the interaction with all the detectors and the action of the final flip (but before the particle passing through the last beam splitter) the global state of the system and detectors reads $|\Psi_f\rangle = [|\psi_1\rangle|a=1\rangle + |\psi_{-1}\rangle|a=-1\rangle]/\sqrt{2}$, where $|\psi_1\rangle = \sum_{\{r_k\}}|\{r_k\}\rangle\mathcal{M}_N^{(r_N)}\ldots\mathcal{M}_1^{(r_1)}|\psi_0\rangle e^{i\gamma}$

and $|\psi_{-1}\rangle = \sum_{\{r_k\}} |\{r_k\}\rangle R^{-1}(\mathbf{n}_0)\sigma_x^{(s)} R(\mathbf{n}_0)\tilde{\mathcal{M}}_N^{(r_N)} \dots \tilde{\mathcal{M}}_1^{(r_1)} R^{-1}(\mathbf{n}_0)\sigma_x^{(s)} R(\mathbf{n}_0)|\psi_0\rangle$, where $|\{r_k\}\rangle$ is the state of the collection of detectors the particle interacted with determined by the readout sequence $\{r_k\}$, γ is an extra phase that controls the interference pattern, and the Kraus operators $\mathcal{M}_k^{(r_k)} = M_{\eta_k}(\mathbf{n}_k, r_k) = R^{-1}(\mathbf{n}_k) M_\eta(\mathbf{e}_z, r_k) R(\mathbf{n}_k)$ and $\tilde{\mathcal{M}}_k^{(r_k)} = M_{\eta_k}(-\mathbf{n}_k, r_k) = R^{-1}(\mathbf{n}_k)\sigma_x^{(s)} M_\eta(\mathbf{e}_z, r_k)\sigma_x^{(s)} R(\mathbf{n}_k)$. The intensity of the output signals at D_1 and D_2 are

$$I_{1,2} = I_0 \langle \Psi_f | (1 \pm \sigma_x^{(a)}) | \Psi_f \rangle / 2.$$

We now employ the fact that the last measurement is projective and postselected to $r_N = +$, with the $r_N = -$ readout not taken into account in calculating $I_{1,2}$. Therefore, $\mathcal{M}_N^{(r_N)} = \mathcal{P}_0 = |\psi_0\rangle\langle\psi_0| = |\mathbf{n}_0\rangle\langle\mathbf{n}_0|$ and $\tilde{\mathcal{M}}_N^{(r_N)} = |-\mathbf{n}_0\rangle\langle -\mathbf{n}_0| = R^{-1}(\mathbf{n}_0)\sigma_x^{(s)} R(\mathbf{n}_0)|\mathbf{n}_0\rangle\langle\mathbf{n}_0| R^{-1}(\mathbf{n}_0)\sigma_x^{(s)} R(\mathbf{n}_0)$, leading to

$$|\psi_1\rangle = \sum_{\{r_k\}} |\{r_k\}\rangle |\psi_0\rangle \times \left(\langle\psi_0| \mathcal{M}_{N-1}^{(r_{N-1})} \dots \mathcal{M}_1^{(r_1)} |\psi_0\rangle e^{i\gamma} \right), \tag{4}$$

$$|\psi_{-1}\rangle = | \sum_{\{r_k\}} |\{r_k\}\rangle |\psi_0\rangle \times \left(\langle\psi_0| R^{-1}(\mathbf{n}_0)\sigma_x^{(s)} R(\mathbf{n}_0) \tilde{\mathcal{M}}_{N-1}^{(r_{N-1})} \dots \tilde{\mathcal{M}}_1^{(r_1)} R^{-1}(\mathbf{n}_0)\sigma_x^{(s)} R(\mathbf{n}_0) |\psi_0\rangle \right). \tag{5}$$

In order to simplify the expression for $|\psi_{-1}\rangle$, we use the property

$$\langle\psi_0| R^{-1}(\mathbf{n}_0)\sigma_x^{(s)} R(\mathbf{n}_0) \tilde{\mathcal{M}}_{N-1}^{(r_{N-1})} \dots \tilde{\mathcal{M}}_1^{(r_1)} R^{-1}(\mathbf{n}_0)\sigma_x^{(s)} R(\mathbf{n}_0) |\psi_0\rangle = \left(\langle\psi_0| \mathcal{M}_{N-1}^{(r_{N-1})} \dots \mathcal{M}_1^{(r_1)} |\psi_0\rangle \right)^*, \tag{6}$$

which we prove hereafter. Then, one immediately arrives at Eq. (2) for $I_{1,2}$.

Computation of the phase accumulated through the lower arm. The evolution of the state through the lower arm entering the intensities at the interferometer drain is computed via the property in Eq. (6), which we prove here. We recall from the Methods in the manuscript (cf. Eqs. (19,20) therein) that

$$\delta R = R(\mathbf{n}_{k+1}) R^{-1}(\mathbf{n}_k) = \begin{pmatrix} \cos^2\frac{\theta}{2} + e^{-2\pi i/N}\sin^2\frac{\theta}{2} & \frac{1}{2}(1 - e^{-2\pi i/N})\sin\theta \\ \frac{1}{2}(1 - e^{-2\pi i/N})\sin\theta & \sin^2\frac{\theta}{2} + e^{-2\pi i/N}\cos^2\frac{\theta}{2} \end{pmatrix}, \tag{7}$$

and

$$M_\eta(\mathbf{e}_z, +) = \begin{pmatrix} 1 & 0 \\ 0 & \sqrt{1-\eta} \end{pmatrix}, \; M_\eta(\mathbf{e}_z, -) = \begin{pmatrix} 0 & 0 \\ 0 & \sqrt{\eta} \end{pmatrix}. \tag{8}$$

Using the hermiticity of $M_\eta(\mathbf{e}_z, r_k)$, and the identities

$$\sigma_x^{(s)} \delta R \sigma_x^{(s)} = e^{-2\pi i/N} \sigma_z^{(s)} \delta R^{-1} \sigma_z^{(s)} = e^{-2\pi i/N} \sigma_z^{(s)} \delta R^\dagger \sigma_z^{(s)}, \tag{9}$$

$$\sigma_z^{(s)} M_\eta(\mathbf{e}_z, r_k) \sigma_z^{(s)} = M_\eta(\mathbf{e}_z, r_k), \tag{10}$$

for δR, we can write

$$\begin{aligned}
&\langle\psi_0| R^{-1}(\mathbf{n}_0)\sigma_x^{(s)} R(\mathbf{n}_0) \tilde{\mathcal{M}}_{N-1}^{(r_{N-1})} \dots \tilde{\mathcal{M}}_1^{(r_1)} R^{-1}(\mathbf{n}_0)\sigma_x^{(s)} R(\mathbf{n}_0) |\psi_0\rangle \\
&\quad = \langle \mathbf{e}_z | \sigma_x^{(s)} \delta R \sigma_x^{(s)} M_\eta(\mathbf{e}_z, r_{N-1}) \sigma_x^{(s)} \delta R \sigma_x^{(s)} M_\eta(\mathbf{e}_z, r_{N-2}) \sigma_x^{(s)} \delta R \dots \delta R \sigma_x^{(s)} M_\eta(\mathbf{e}_z, r_1) \sigma_x^{(s)} \delta R \sigma_x^{(s)} | \mathbf{e}_z \rangle \\
&\quad = e^{-2\pi i N/N} \langle \mathbf{e}_z | \sigma_z^{(s)} \delta R^\dagger \sigma_z^{(s)} M_\eta(\mathbf{e}_z, r_{N-1}) \sigma_z^{(s)} \delta R^\dagger \dots \delta R^\dagger \sigma_z^{(s)} M_\eta(\mathbf{e}_z, r_1) \sigma_z^{(s)} \delta R^\dagger \sigma_z^{(s)} | \mathbf{e}_z \rangle \\
&\quad = \langle \mathbf{e}_z | \delta R^\dagger M_\eta(\mathbf{e}_z, r_{N-1}) \delta R^\dagger M_\eta(\mathbf{e}_z, r_{N-2}) \delta R^\dagger \dots \delta R^\dagger M_\eta(\mathbf{e}_z, r_1) \delta R^\dagger | \mathbf{e}_z \rangle \\
&\quad = \left(\langle \mathbf{e}_z | \delta R M_\eta(\mathbf{e}_z, r_1) \delta R M_\eta(\mathbf{e}_z, r_2) \delta R \dots \delta R M_\eta(\mathbf{e}_z, r_{N-1}) \delta R | \mathbf{e}_z \rangle \right)^*.
\end{aligned} \tag{11}$$

Using the explicit representation of

$$|\mathbf{e}_z\rangle = \begin{pmatrix} 1 \\ 0 \end{pmatrix}, \tag{12}$$

(cf. Eq. (14) in the manuscript), we consider

$$\begin{aligned}
&\langle \mathbf{e}_z | \delta R M_\eta(\mathbf{e}_z, r_1) \delta R M_\eta(\mathbf{e}_z, r_2) \delta R \dots \delta R M_\eta(\mathbf{e}_z, r_{N-1}) \delta R | \mathbf{e}_z \rangle \\
&\quad = \left(\langle \mathbf{e}_z | \delta R M_\eta(\mathbf{e}_z, r_1) \delta R M_\eta(\mathbf{e}_z, r_2) \delta R \dots \delta R M_\eta(\mathbf{e}_z, r_{N-1}) \delta R | \mathbf{e}_z \rangle \right)^T \\
&\quad = \langle \mathbf{e}_z | \delta R M_\eta(\mathbf{e}_z, r_{N-1}) \delta R M_\eta(\mathbf{e}_z, r_{N-2}) \delta R \dots \delta R M_\eta(\mathbf{e}_z, r_1) \delta R | \mathbf{e}_z \rangle,
\end{aligned} \tag{13}$$

where T denotes transposition, and in the last step we used $\delta R^T = \delta R$ and $M_\eta(\mathbf{e}_z, r)^T = M_\eta(\mathbf{e}_z, r)$, cf. (7, 8). Finally, noticing that

$$\langle \mathbf{e}_z | \delta R M_\eta(\mathbf{e}_z, r_{N-1}) \delta R M_\eta(\mathbf{e}_z, r_{N-2}) \delta R ... \delta R M_\eta(\mathbf{e}_z, r_1) \delta R | \mathbf{e}_z \rangle = \langle \psi_0 | \mathcal{M}_{N-1}^{(r_{N-1})} \dots \mathcal{M}_1^{(r_1)} | \psi_0 \rangle, \tag{14}$$

one obtains Eq. (6), as desired.